Article ID: 1000-7032(2025)07-1271-12

Optical Spectroscopy Methods for Determining Semiconductor Bandgaps

ZHANG Yong*

(*Department of Electrical and Computer Engineering, University of North Carolina at Charlotte, Charlotte, NC* 28223, *USA*)

* *Corresponding Author, E-mail: yong. zhang@charlotte. edu*

Abstract: Although there are numerous optical spectroscopy techniques and methods that have been used to extract the fundamental bandgap of a semiconductor, most of them belong to one of these three approaches: (1) the excitonic absorption, (2) modulation spectroscopy, and (3) the most widely used Tauc-plot. The excitonic absorption is based on a many-particle theory, which is physically the most correct approach, but requires more stringent crystalline quality and appropriate sample preparation and experimental implementation. The Tauc-plot is based on a single-particle theory that neglects the many-electron effects. Modulation spectroscopy analyzes the spectroscopy features in the derivative spectrum, typically, of the reflectance and transmission under an external perturbation. Empirically, the bandgap energy derived from the three approaches follow the order of $E_{ex} > E_{MS} > E_{TP}$, where three transition energies are from excitonic absorption, modulation spectroscopy, and Tauc-plot, respectively. In principle, defining E_g as the single-electron bandgap, we expect $E_g > E_{ex}$, thus, $E_g > E_{TP}$. In the literature, E_{TP} is often interpreted as E_g, which is conceptually problematic. However, in many cases, because the excitonic peaks are not readily identifiable, the inconsistency between E_g and E_{TP} becomes invisible. In this brief review, real world examples are used (1) to illustrate how excitonic absorption features depend sensitively on the sample and measurement conditions; (2) to demonstrate the differences between E_{ex}, E_{MS}, and E_{TP} when they can be extracted simultaneously for one sample; and (3) to show how the popularly adopted Tauc-plot could lead to misleading results. Finally, it is pointed out that if the excitonic absorption is not observable, the modulation spectroscopy can often yield a more useful and reasonable bandgap than Tauc-plot.

Key words: semiconductor material; bandgap; excitonic absorption; modulation spectroscopy; Tauc plot

CLC number: TN304 **Document code**: A

DOI: 10. 37188/CJL. EN20240013 **CSTR**: 32170. 14. CJL. EN20240013

确定半导体禁带宽度的光谱方法

张 勇*

(*Department of Electrical and Computer Engineering, University of North Carolina at Charlotte, Charlotte, NC* 28223, *USA*)

摘要: 尽管有多种光谱技术可用来提取半导体的禁带宽度或带隙,但它们大多属于以下三种方法之一:(1)激子吸收,(2)调制光谱,(3)最广泛使用的 Tauc 图。激子吸收基于多粒子理论,在物理意义上是最明确的,但对晶体质量、样品制备和实验实施有更高的要求。Tauc 图基于单粒子理论,忽略了多电子效应。调制光谱分析反射和透射在外部微扰下的微分光谱特征。经验上,从这三种方法得到的带隙能量按顺序为 $E_{ex} > E_{MS} > E_{TP}$,其中 3 个跃迁能量分别来自激子吸收、调制光谱和 Tauc 图。原则上,如果定义 E_g 为单电子带隙,我们期望 $E_g > E_{ex}$,因此,$E_g > E_{TP}$。在文献中,E_{TP} 通常被解释为 E_g,这在概念上是有问题的。然而,在许多情况下,由于激子吸收峰不容易被观测到,人们意识不到 E_g 和 E_{TP} 之间的不一致问题。这篇简短的综述使用真实样品的例子,

收稿日期: 2024-10-10; **修订日期**: 2024-12-23

基金项目: 北卡罗来纳大学夏洛特分校 Bissell 杰出教授捐赠基金

Supported by Bissell Distinguished Professor Endowment Fund at UNC-Charlotte

(1)说明激子吸收特征如何依赖于样品和测量条件;(2)展示当它们可以同时提取时,E_{ex}、E_{MS}和E_{TP}之间的差异;(3)演示广泛采用的Tauc图如何可能导致误导性的结果。最后指出,如果不能观察到激子吸收峰,调制光谱通常可以比Tauc图得到更有用和合理的带隙。

关 键 词: 半导体材料; 禁带宽度; 激子吸收; 调制光谱; Tauc图

1 Introduction

Many spectroscopy techniques are used to determine the bandgaps of semiconductors, such as optical absorption, reflectance, modulation spectroscopy, photoluminescence, photo-response, optical diffuse reflectance. On the other hand, different theoretical models are used to extract the bandgap value from the experimental data. These theoretical modes are built upon different levels of electronic band structure theories. Although they may defer in detail, the most major difference among them is whether they are based on a single-electron (or quasi-particle) theory or many-particle (*i. e.*, excitonic) theory.

Optical properties are closely related to the dielectric function of the material that includes the real and imaginary part. Experimentally measured optical properties naturally reflect the many-particle effects, but properly including the many-particle effects in the theoretical modeling is often non-trivial.

The electronic density of states (DOS) near critical points plays a pivotal role in determining the optical properties of the material. For a three-dimensional (3D) isotropic semiconductor, with a parabolic dispersion $E(\boldsymbol{k}) = \hbar^2\boldsymbol{k}^2/(2m^*)$, the DOS is given as:

$$\rho(E) = \frac{m^*[2m^*(E - E_0)]^{1/2}}{\pi^2\hbar^3}, \tag{1}$$

where m^* is the effective mass and E_0 is the band edge energy. Eq. (1) is valid for $E > E_0$, whereas for $E < E_0$, $\rho(E) = 0$. This functional form is derived within the framework of the single particle theory. A key signature of this DOS is its square-root dependence on $E - E_0$ with $\rho(E_0) = 0$, which dictates the functional form of the absorption spectrum based on the single-particle theory.

The absorption coefficient function $\alpha(\omega)$ is often expressed in terms of the extinction coefficient $K(\omega)$ or imaginary part of the dielectric function $\varepsilon_2(\omega)$ through the formula below[1]:

$$\alpha(\omega) = \frac{2\omega K(\omega)}{c} = \frac{\omega}{n(\omega)c}\varepsilon_2(\omega), \tag{2}$$

where $n(\omega)$ is the refractive index. Although its frequency dependence is often neglected, in fact, $n(\omega)$ can have a maximum near the bandgap[2-3]. While $K(\omega)$ is more directly related to the attenuation of light passing through the material, $\varepsilon_2(\omega)$ is more convenient to be calculated from the electronic band structure. Often, $\varepsilon_2(\omega)$ is treated as equivalent to the absorption coefficient in the literature, but we should not forget the contribution of $n(\omega)$.

In the single-particle framework and dipole approximation, for a direct band-gap semiconductor, the inter-band optical transition between the valance band (VB) and conduction band (CB) yields $\varepsilon_2(\omega)$ below[1]:

$$\varepsilon_2(\omega) = 0, \text{ for } \hbar\omega < E_g,$$
$$\varepsilon_2(\omega) = \frac{2\pi e^2}{m^2\omega^2}\left|\boldsymbol{e}\cdot\boldsymbol{M}_{cv}(0)\right|^2\left(\frac{2\mu}{\hbar^2}\right)^{3/2}(\hbar\omega - E_g)^{1/2}, \text{ for } \hbar\omega > E_g, \tag{3}$$

where $\hbar\omega$ is the photon energy, E_g=E_c−E_v the fundamental bandgap, $\mu = \frac{m_c^* m_v^*}{m_c^* + m_v^*}$ the reduced mass, $\boldsymbol{e}$ the polarization of the light, $\boldsymbol{M}_{cv}(0)$ is the dipole matrix element between the CB and VB band edge states at $k = 0$. Here we only consider the allowed transition (*i. e.*, $\boldsymbol{M}_{cv}(0) \neq 0$)[1]. The key signature of this function is the square-root dependence that indicates zero absorption at $\hbar\omega = E_g$.

Within the same general approach but for an indirect bandgap material, for the inter-band transition involving a phonon emission process, $\varepsilon_2(\omega)$ is given as[1]:

$$\varepsilon_{2,abs}(\omega) = 0, \text{ for } \hbar\omega < E_g - k\theta,$$
$$\varepsilon_{2,abs}(\omega) = C_1(\hbar\omega - E_g + k\theta)^2 n_{q0}, \text{ for } \hbar\omega > E_g - k\theta, \tag{4}$$

where $k\theta$ is the energy of the phonon at a wavevector

$\boldsymbol{q}_0$ at which the indirect band edge locates, n_{q0} is the average phonon occupation number, and C_1 is a constant.

For the process involving the emission of a phonon, we have[1]:

$$\varepsilon_{2,\mathrm{emiss}}(\omega) = 0, \text{ for } \hbar\omega < E_g + k\theta,$$
$$\varepsilon_{2,\mathrm{emiss}}(\omega) = C_2(\hbar\omega - E_g - k\theta)^2(n_{q0} + 1), \text{ for } \hbar\omega > E_g + k\theta, \quad (5)$$

where C_2 is a constant. The key signature of Eqs. (4) or (5) is the square dependence that indicates zero absorption at $\hbar\omega = E_g \pm k\theta$.

Eqs. (3)-(5) are the foundation for the widely used Tauc-plot scheme[4] and other related ones (*e. g.*, the Kubelka-Munk function for the diffuse reflectance analysis[5]) for determining the bandgap of a semiconductor from its absorption spectrum. Unfortunately, this scheme is a highly problematic practice, which will be discussed below.

When the many-body or excitonic effect is considered, the absorption spectrum becomes drastically different from that described by either Eq. (3) or Eq. (4)-(5). In a nutshell, the excitonic effect is a change in the total Coulomb and exchange interactions between the ground and excited state of the many-electron system. The ground state is referred to as that when all electrons are in the VB, and the excited state when one electron is excited to the CB while the rest remain in the VB. When the excitonic effect is relatively weak (commonly referred to as a Wannier exciton), the exciton problem can be simplified to a hydrogenic model with a screened Coulomb interaction between an electron in the CB and a hole in the VB moving with the respective effective masses. For an isotropic 3D material, the optical transition energies of the discrete excitonic states are given as[1]:

$$E_{ex} = E_g - \frac{R}{n^2}, \quad (6)$$

where $R = (\mu e^4)/(2\hbar^2\varepsilon^2)$ is the effective Rydberg.

In most inorganic semiconductors, because the exciton binding energy $E_b = R$ is relatively small, typically in the order of a few to a few tens meV, the modification in the position of the energy threshold in the optical absorption spectrum is indeed relatively small. However, it is inappropriate to further argue that the excitonic effect is also small in the absorption spectrum to justify the use of the single-particle formalisms of Eqs. (3)-(5). As a matter of fact, for GaAs with E_b being merely 4.2 meV, the low temperature absorption at the excitonic peak E_{ex} may exceed 5×10^4 cm^{-1}, in contrast to zero at E_g according to the single particle theory.

The imaginary part of the dielectric function with the excitonic effect included, as shown schematically by Fig. 1, is given below[6]:

$$\varepsilon_2(\omega) = \varepsilon_{2F}(\omega)\frac{\pi x e^{\pi x}}{\sinh(\pi x)}, \quad (7)$$

where $x = \sqrt{R/(\hbar\omega - E_g)}$, and $\varepsilon_{2F}(\omega)$ is the function of the single-electron theory, Eq. (3). Now the absorption at the bandgap E_g is non-zero but finite: when $\hbar\omega$ is greater but close to E_g, $\varepsilon_2(\omega) \approx 2\pi x \cdot \varepsilon_{2F}(\omega) \propto |\boldsymbol{M}_{cv}(0)|^2\sqrt{R}$. Eq. (7) indicates that the excitonic effect does not vanish even well above E_g. Only when $x \ll 1$ or $\hbar\omega - E_g \gg R$, $\varepsilon_2(\omega) \to \varepsilon_{2F}(\omega)$.

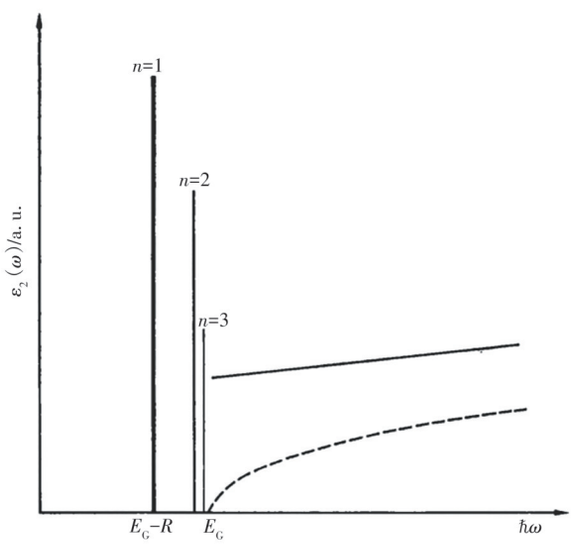

Fig. 1　Schematic diagram of the imaginary part of the dielectric function, $\varepsilon_2(\omega)$, for the dipole allowed optical transition with inclusion of excitonic effects. The dashed line indicates $\varepsilon_2(\omega)$ neglecting the excitonic effects[1]

2　Excitonic Absorption in a Prototype Semiconductor GaAs

Appropriate sample selection and preparation and using a suitable measurement technique are critical to observe the excitonic absorption peaks in a

semiconductor.

Among the familiar group Ⅳ and Ⅲ - Ⅴ semiconductors, the excitonic absorption was perhaps first observed in an indirect semiconductor Ge near its direct bandgap in 1958[7], as shown in Fig. 2(a) for a 10 μm thick sample. The absorption coefficient at the excitonic peak $\alpha(E_{ex})$ is about 4.1×10^3 cm^{-1} at 20 K with $E_b \approx 1$ meV[7]. Interestingly, even at room temperature (291 K), one could still see the vestige of the excitonic peak.

For the direct bandgap semiconductors, the excitonic absorption was first observed in Cu_2O in 1950[8], which was also perhaps the first report of excitonic absorption in a semiconductor. As shown in Fig. 2(b), the low-temperature absorption spectrum shows many excitonic peaks up to $n = 25$, with $E_b = 92$ meV [9]. However, the $n = 1$ peak at the excitonic bandgap E_{ex}=2.080 eV is missing, because Cu_2O has inversion symmetry and the $n = 1$ excitonic transition is parity forbidden for the dipole transition[1].

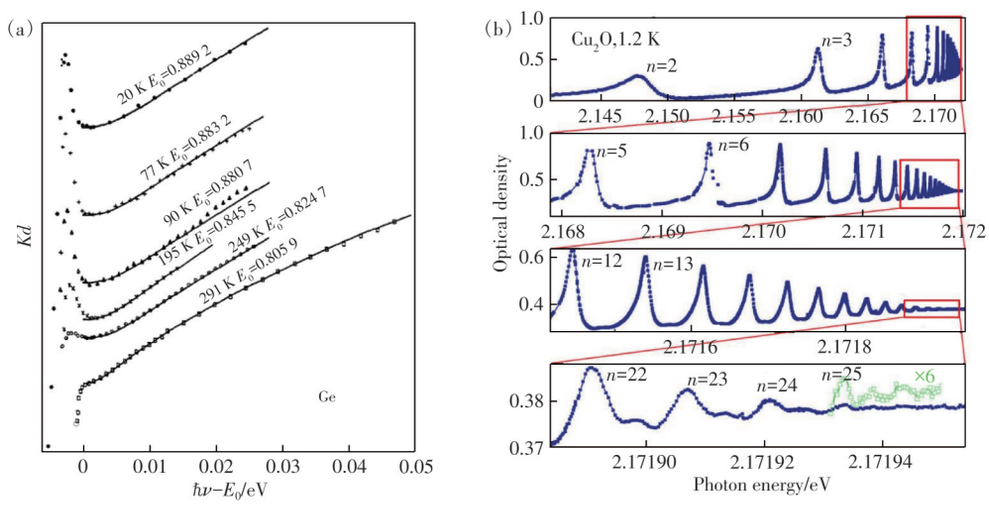

Fig. 2 Absorption spectra of Ge and CuO_2, showing excitonic absorption peaks. (a)Ge between 20 K and 291 K (the energy reference is the direct bandgap energy E_0 at 20 K)[7]. (b)CuO_2 at 1.2 K[9]

Among the direct bandgap semiconductors with an allowed, band-edge excitonic dipole transition, the excitonic absorption was first reported for GaAs in 1961[10-11], with the spectrum shown in Fig. 3(a) (for a mechanically thinned, 6.5 μm thick sample)[11]. This is a seminal spectrum for the excitonic absorption that appears in many textbooks. This spectrum shows an excitonic bandgap $E_{ex} = 1.513$ eV, and a peak absorption $\alpha(E_{ex}) \sim 1.13\times10^4$ cm^{-1}. More precise measurements have become available thereafter, such as the one shown in Fig. 3(b) (for a 1 μm thick epilayer)[12], where the $n = 3$ excitonic peak is resolved. The 1s exciton energy and exciton binding energy have been precisely determined as 1.515 2 eV and $E_b = 4.2$ meV[13]. Interestingly, Fig. 3(b) also exhibits absorption peaks associated with impurities below the 1s excitonic peak. These peaks will merge with the main excitonic peak at higher temperatures as tail absorption. The absorption strength of the 1s peak was found to be $(2-3)\times10^4$ cm^{-1}[12-13] that was not able to be obtained very accurately due to the saturation of the detection system[13] (the limitation of the dynamic range of the detector). Another later measurement seems to show a somewhat stronger peak absorption > 4×10^4 cm^{-1} (for a 1 μm thick lift-off epilayer), as shown in Fig. 3(c)[14]. Stronger excitonic absorption has been reported for some bulk Ⅱ - Ⅵ compounds, such as ZnTe, ~1.4×10^5 cm^{-1}[15]; and organic-inorganic hybrid $ZnTe(en)_{0.5}$, estimated to be > 10^6 cm^{-1}[16], likely the strongest band-edge excitonic emission among semiconductors.

One might have seen a plausible argument that because the exciton binding energy of GaAs is much smaller than the thermal energy kT at room temperature, the excitonic effect would vanish at room temperature. Actually, the excitonic absorption peak, albeit being rather feeble, remains observable even at room temperature, resulting in $E_{ex} = 1.425$ eV, as

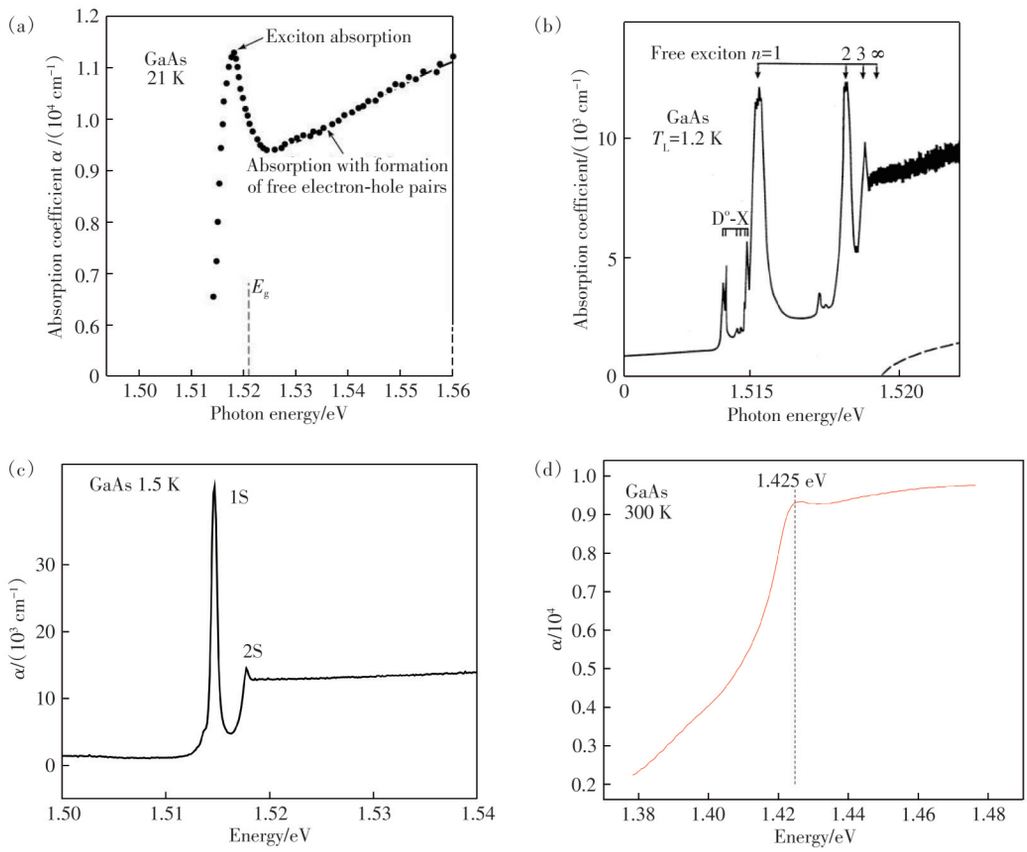

Fig. 3　Absorption spectra of GaAs measured at different conditions, showing the band edge excitonic absorption peak(s): (a)at 21 K[11], (b)1.2 K[12], (c)1.5 K[14], (d)300 K[17]

shown in Fig. 3(d)[17]. Here, the absorption tail below E_{ex} could originate from either the impurity absorption or scattering loss in the measurement. If applying Tauc-plot to the spectrum, one would get a significantly lower bandgap E_g.

While empirically the peak absorption strength seems to positively correlate with the exciton binding energy, a reliable theory that can accurately predict the strength of the intrinsic exciton absorption peak at the 0 K limit is not yet available to the best knowledge of the author. One could understand that the excitonic absorption reflects some sort of coherently enhanced interference effect of excited electronic waves. The dephasing effects, such as electron-phonon interaction at an elevated temperature, can lead to the reduction in the peak strength and broadening of the peak width of the excitonic absorption. However, the impact of the temperature cannot simply be gauged by the relative value of E_b/kT.

In summary, in a high crystallinity sample, the excitonic absorption can offer an unambiguous and very accurate excitonic bandgap (with an uncertainty in the order of 0.1 meV due to the calibration of the spectroscopy system and/or residual strain in the sample). However, the accurate absorption strength still exhibits considerable uncertainty even for an as extensively studied material as GaAs. Evidently, for the examples mentioned above, it make no sense to use the single-particle theory like Eq. (3) or Tauc plot, to identify their bandgaps.

3　Impact of Structural Imperfection on the Excitonic Absorption Spectrum

The presence of a sharp excitonic absorption peak is a useful and sensitive indicator for the high level of crystallinity that manifests as a well-defined (excitonic) bandgap. Various forms of structural imperfections, such as doping, alloying, and lattice vibrations at elevated temperatures, may diminish the excitonic peak.

Nitrogen doped GaAs (GaAs:N) or dilute nitride alloys ($GaAs_{1-x}N_x$) may serve as good prototypes

to show these effects[14], and illustrate how different measurement techniques can yield different bandgaps and how to put them in perspective. This material system is a nice example for the so-called highly mismatched alloys, because of the large size and chemical differences between N and As. As shown in Fig. 4[14], a red shift in a fraction of 1 meV is observable for a nitrogen composition x_N as low as 10^{-5}, showing that the excitonic absorption peak can be used for very precise monitoring of the band structure change due to impurity doping. With increasing x_N, the alloy exhibits further red shift in the bandgap, accompanied by the linewidth broadening. Particularly, for $x_N > 0.1\%$ ([N] > 2×10^{19} cm^{-3}), the excitonic peak decreases severely, and is nearly washed out when x_N is close to 0.4% ([N] ~ 10^{20} cm^{-3}). Apparently, for this particular material system, $x_N \sim 0.4\%$ is about the highest composition at which the excitonic absorption peak is still identifiable (at 1.426 eV) at 1.5 K. In this situation, without systematically monitoring the evolution with varying x_N, most people would probably use the Tauc plot to determine the bandgap, as commonly seen in the literature. Applying the Tauc plot would yield a band gap about 15 meV lower than the excitonic bandgap. This special composition serves the purpose to show that the bandgap from the Tauc plot is not what the model intends to give, because the Tauc plot is supposed to yield the single-particle bandgap that should be above the excitonic bandgap instead of below it.

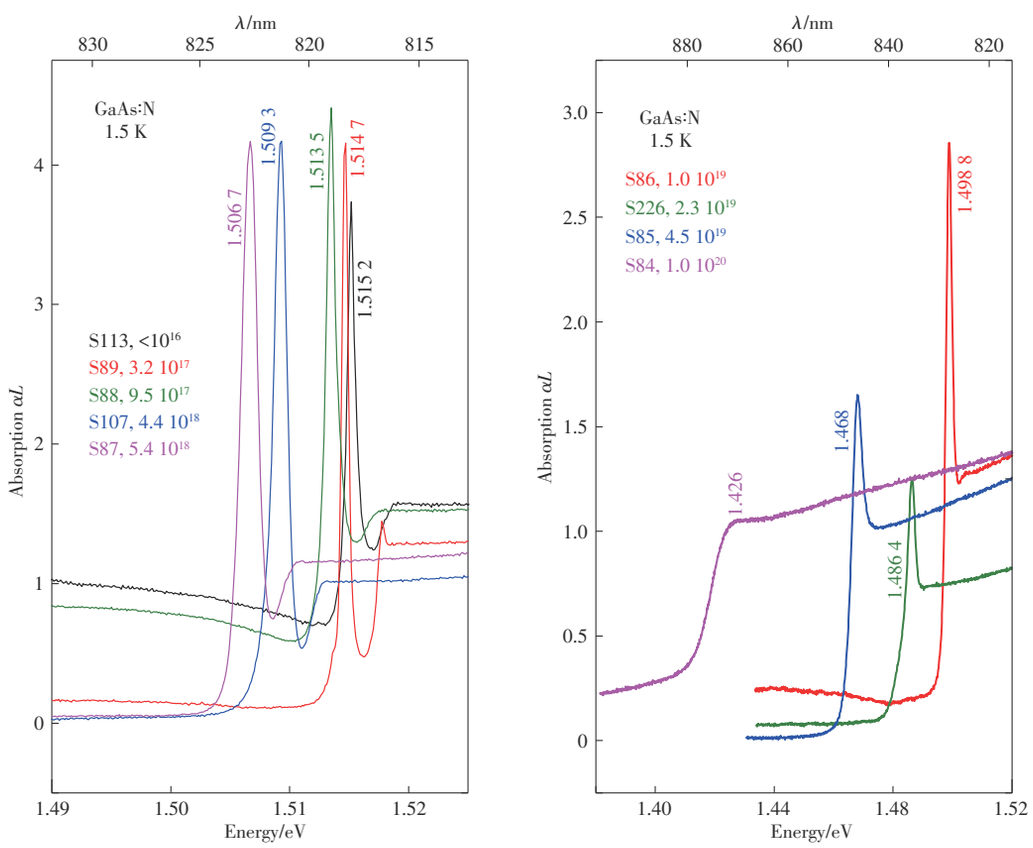

Fig. 4 Low temperature absorption spectra of free-standing GaAs:N films with varying nitrogen doping level[14]

Fig. 5(a) offers an example of a conventional alloy system $Ga_{1-x}In_xP$, where the atomic differences between Ga and In are relatively small. In this case, even for $x \sim 0.5$ (where the alloy disordering effects are expected to be almost the strongest), the excitonic absorption peak remains clearly visible at low temperatures (*e. g.*, 5 K)[14], despite much weaker and broader, compared to those of GaAs measured at the comparable temperatures, such as Fig. 3(b) and 3(c). Also included is a photo-absorption spectrum of the same sample, yielding a bandgap slightly below the excitonic peak. Fig. 5(b) gives a similar comparison for GaAs[17]. More discussion about the modulation spectroscopy will be given in the next section.

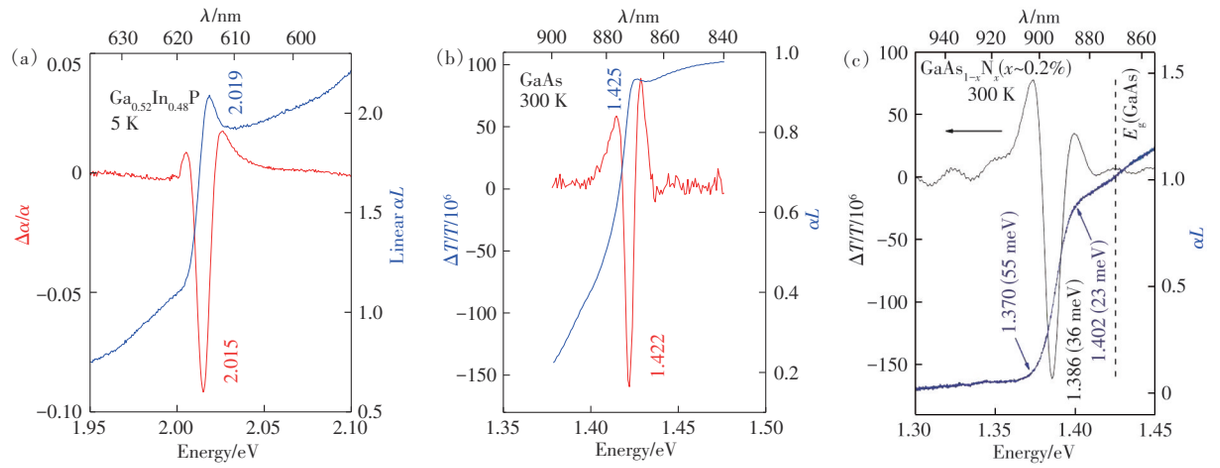

Fig. 5　Comparison of absorption and modulation (photo-absorption) spectroscopy results. (a) $Ga_{0.52}In_{0.48}P$ at 5 K[14], (b) GaAs at 300 K[17], and (c) $GaAs_{1-x}N_x$ (actual x ~ 0.08% instead of nominal value 0.2%) at 300 K[17]

For a small bandgap semiconductor, because of a small exciton binding energy associated with a reduction in the effective mass of the electron and an increase in the static dielectric constant, the excitonic feature of the intrinsic absorption spectrum near the fundamental band edge can be more easily smeared out by various extrinsic effects. These effects may include the screening by free carriers, ionization by an electric field, and broadening by the random field of impurities, inhomogeneous strain, or thermal vibrations. For instance, for InAs with $R \approx 1.7$ meV[18] and InSb with $R \approx 0.5$ meV[19], only in high purity and quality samples, their excitonic absorption peak can be observed. Shown in Fig. 6 are the absorption spectra of InSb measured at low temperatures under different sample and measurement conditions. Fig. 6(a) is for a supposedly pure InSb measured at 5 K[20-21], there no excitonic peak is observable. Fig. 6(b) shows the spectra measured at 2 K for a weakly doped p-type sample with $p = 6\times10^{12}$ cm^{-3} at 77 K, where the spectrum #1 is for the as-grown sample (without any observable excitonic peak), #2 for an annealed sample, showing an excitonic peak, and #3−#5 for the as-grown sample but measured under 4 000, 7 200, 10 000 A/m (50, 90, 125 Oe) magnetic field, respectively[19]. Presumably, annealing improves the crystallinity (#2), and magnetic confinement reduces the exciton Bohr radius (#3−#5), both favoring the observation of the excitonic peak. When the Debye length, defined as $L_D = \sqrt{\epsilon_0 \epsilon k_B T/(q^2 n)}$, is smaller than the Bohr radius, the Coulomb interaction between the electron and hole of the exciton will be screened[21]. Thus, low temperature and low doping level are necessary to preserve the excitonic absorption peak for a semiconductor with a small bandgap, even it is a binary. For instance, for InSb, it is suggested that $N_A + N_D$ should not exceed 2×10^{14} cm^{-3}[19] to see the excitonic peak. Unfortunately, the spectrum of Fig. 6(a) is adopted in a widely used textbook as an example of a pure direct bandgap semiconductor[22], which enforces the wrong impression that Tauc-plot is a reliable way for determining the bandgap. Understandably, with the absorption spectrum like Fig. 6(a), one would attempt to extract the bandgap from the absorption threshold by fitting to a Tauc-plot like function. However, doing so would yield a free-electron bandgap E_g below that of the free exciton.

Similar situations may occur for higher bandgap semiconductors. For instance, for GaN, the excitonic absorption peak can be observed at room temperature in a low doped sample, as shown in Fig. 6(c) for a unintentionally n-type doped 0.4-μm-thick GaN film (with a free electron concentration of 10^{17} cm^{-3}) grown by MOCVD on a c-plane sapphire substrate[23]. The excitonic peak is found at 3.432 eV (slightly affected by the epitaxial strain) with an estimated exciton binding energy of about 20 meV, and the corresponding bandgap E_g = 3.452 eV is larger than the generally accepted value of ~3.4 eV from

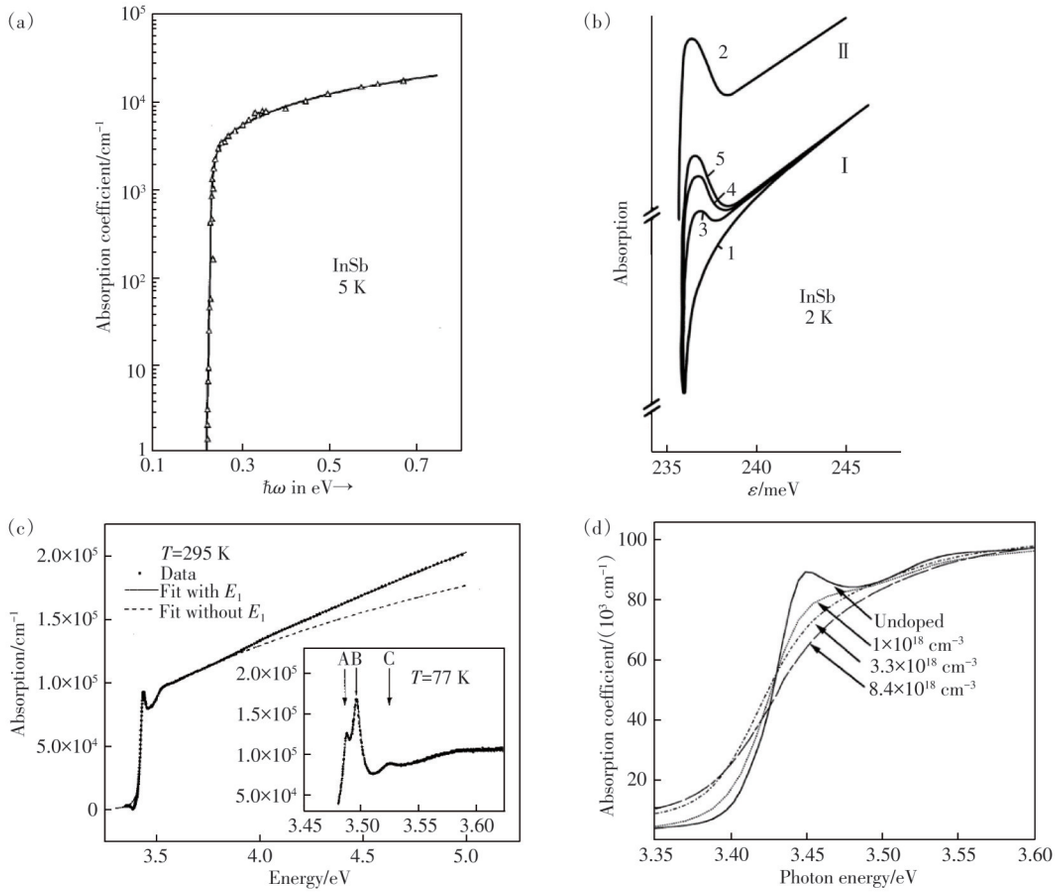

Fig. 6 Absorption spectra of different sample and measurement conditions. (a) and (b) for InSb: (a) a supposedly pure sample measured at 5 K[20]; and (b) at 2 K (#1: as-grown sample, #2: annealed sample, #3–#5: as-grown samples with different applied magnetic fields)[19]. (c) and (d) for GaN at room temperature: (c) an unintentionally doped sample with a low free carrier concentration[23]; (d) undoped and highly doped samples[24]

Tauc-plot[23]. Doping is found to smear out the excitonic peak, as shown in Fig. 6(d) for similar samples (0.25-μm-thick) with changing the n-type doing level[24].

4 Modulation Spectroscopy

Various type of modulation spectroscopy techniques, such as electro-reflectance/transmission and photo-reflectance/transmission, are often used to determine the transition energies of the critical points in semiconductors, including the fundamental bandgap[25-26]. Since both reflectance (R) and transmission (T) are related to the real part (ε_1) and imaginary part (ε_2) of the dielectric function, an external electric field or applied light beam may induce changes in the dielectric function, resulting in $\Delta\varepsilon_1$ and $\Delta\varepsilon_2$, which in turns induce changes in reflectance ΔR and transmission ΔT. The spectra of $\Delta R/R$ and $\Delta T/T$ or $\Delta\alpha/\alpha$ are not the same as the spectra of R and T or α.

For an undoped or weakly doped sample, the line-shape of the modulation spectroscopy signal can often be described by a third-derivative function[25]. For a high crystalline quality sample, the bandgap derived from the modulation spectroscopy is often very close to but slightly below the excitonic bandgap, as illustrated by the examples of Fig. 5(a) for $Ga_{1-x}In_xP$ at 5 K: 2.015 eV *vs.* 2.019 eV[14]; Fig. 5(b) for GaAs at 300 K: 1.422 eV *vs.* 1.425 eV[17]. However, for a more strongly disorder sample, the bandgap obtained from the modulation spectroscopy could be significantly different from that from the excitonic absorption peak[17]. Fig. 5(c) compares the modulation spectrum with the absorption spectrum measured at 300 K for a $GaAs_{1-x}N_x$ sample with a nominal value of $x \approx 0.2\%$ (the actual value around

0.08%). In this case, because of the thermal broadening effect, the excitonic peak has been smeared out. Nevertheless, using the correlation between the bandgap reductions derived from the modulation spectroscopy (at 300 K) and absorption spectroscopy (at 1.5 K), one could estimate the would-be room-temperature excitonic bandgap to be $E_{ex}\approx$ 1.402 eV, compared to the bandgap of E_{MS} = 1.386 eV from the modulation spectroscopy, and that from Tauc plot $E_{TP}\approx$ 1.370 eV.

For a doped sample, the electric field in the surface depletion layer often leads to Franz-Keldysh oscillations (FKOs). The $\Delta R/R$ spectrum can be fitted to a generalized FKO line-shape function with a broadening parameter to extract the bandgap and surface field[27]. Fig. 7 shows such two examples. Fig. 7(a) is an electro-reflectance spectrum, measured at 300 K, for a doped GaAs, and the fitting yields a bandgap E_g = 1.426 eV and surface field = 15.2 kV/cm (Yong Zhang, unpublished results). Fig. 7(b) is the 300 K photo-reflectance spectrum for a CdTe thin film solar cell with a CdS window layer. The fitting results in a bandgap E_g=1.448 eV (lower than that for a pure CdTe, 1.508 eV) and surface field E=31.9 kV/cm[28]. These results offered the confirmation of that the CdTe/CdS p-n junction consists of an intermixed CdTeS alloy layer and an estimate for the corresponding junction field.

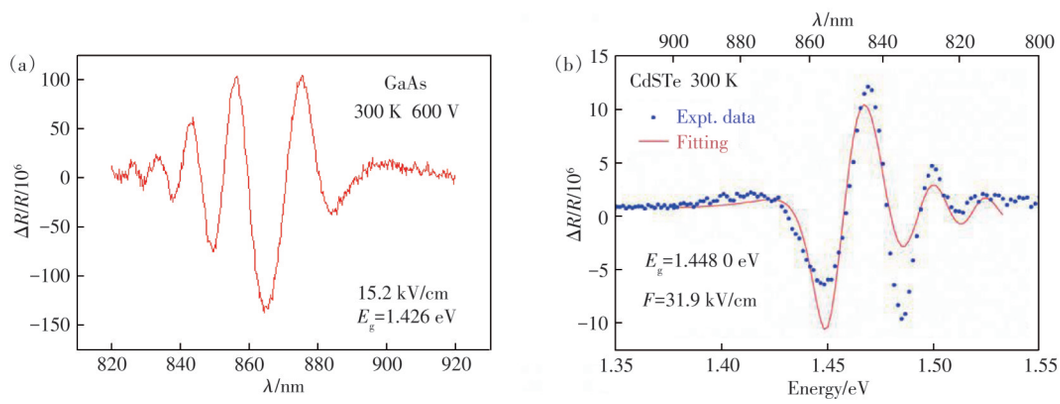

Fig. 7　Examples of modulation spectroscopy data showing Franz-Keldysh oscillations. (a) A contactless electro-reflectance spectrum of a doped GaAs sample. (b) A photo-reflectance spectrum of a CdTe thin-film solar cell with a CdTe/CdS p-n junction[28]

5　Tauc Plot

The Tauc plot[4], based on Eq. (3) or (4)-(5), is widely used to extract the bandgap from absorption spectra. As mentioned above, this practice is conceptually problematic. Evidently, for the cases where excitonic absorption peaks are clearly identifiable, such as for the spectra of Fig. 5(a) and 5(b), using Tauc-plot to extract the bandgap would lead to a single-electron bandgap E_g below the excitonic bandgap E_{ex}, which is contradicting to the original meaning of E_g that is supposed to be above E_{ex}. It is also practically problematic using Tauc-plot to determine the bandgap. On the one hand, it will yield different bandgaps due to different spectral regions used for performing the extrapolation[14,29-30]; and on the other hand, when a thick sample is used, Tauc-plot can lead to a substantially small bandgap due to the tail absorption. Such tail absorption is known to exist even in the absorption measurement of a conventional semiconductor, such as GaAs, where the tail absorption below the excitonic bandgap was specifically studied. It was shown that increasing sample thickness progressively extended the absorption range or measurable absorbance to the longer wavelength side, as shown in Fig. 8(a)[11]. Presumably, the below-bandgap tail shown in Fig. 8(a) is due to the impurity absorption[11]. However, in the literature, Tauc-plot was also used to determine the bandgaps of different GaAs samples, for instance, as shown in Fig. 8(b) for a p-type (1×10^{17} cm^{-3}) GaAs

that shows a bandgap of 1.39 eV at room temperature[31]. This value is substantially smaller than the room temperature excitonic bandgap of 1.425 eV[17], as shown in Fig. 5(b).

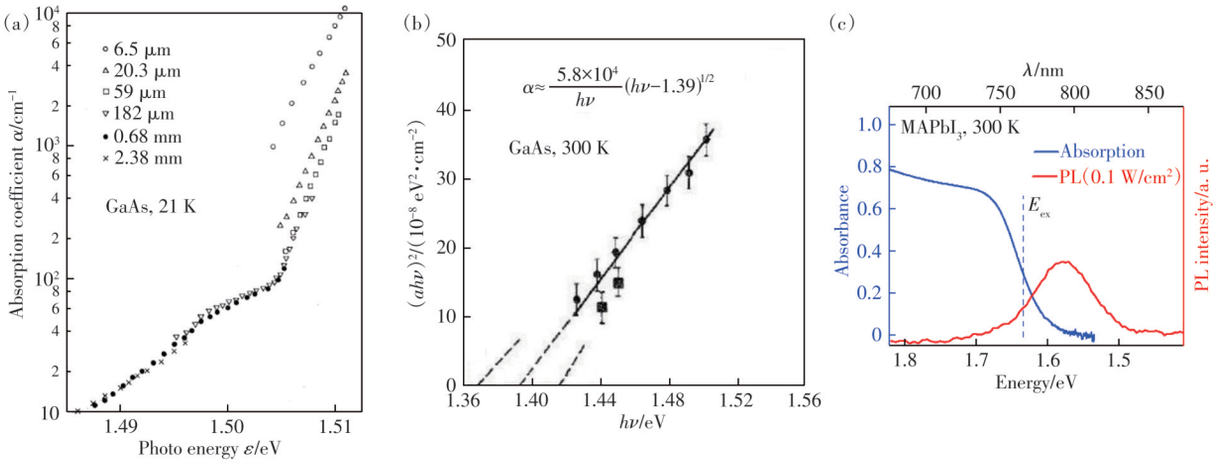

Fig. 8 Examples showing applying the Tauc-plot scheme would result in problematic bandgaps. (a)The absorption below the excitonic bandgap measured by using samples of different thicknesses for GaAs[11]. (b)An underestimate GaAs bandgap using Tauc-plot[31]. (c)Comparison between the absorption and PL spectra of a single crystalline $MAPbI_3$, where the vertical dashed line indicates the estimated free-exciton energy[30]

Although it is useful to examine the absorption tail to assess the threshold wavelength at which the absorbance reaches a specific level (*e. g.*, 1%) for a particular application, one should be caution not to arrive at erroneous and misleading conclusions. For instance, in the recent studies of organic-inorganic halide perovskites, there are some reports about sample thickness dependent bandgaps and photoluminescence (PL) peak above the bandgap[32-35]. It has also been found that the bandgap obtained from Tauc-plot is problematic to be used for assessing the solar cell performance in terms of its short circuit current and open circuit voltage (*e. g.*, an open-circuit voltage unreasonably close to even above the bandgap), and instead, the bandgap derived from the inflection points on the absorption profile is found to be more appropriate[36]. In fact, the "inflection point" scheme is similar to the modulation spectroscopy method. For $MAPbI_3$, the excitonic absorption peak is not observable at room temperature but can be estimated as E_{ex} = 1.634 eV by extrapolating the excitonic bandgap values at lower temperatures to 300 K[37], see Fig. 8(c). On the other hand, the modulation (electro-absorption) or derivative spectroscopy has yielded a bandgap of 1.633 eV[38] or 1.61 eV[29] that is close to the estimated excitonic bandgap[30]. Therefore, instead of attempting to optimize the procedure of applying the Tauc-plot scheme (*e. g.*, subtracting the background[39]), one should do the best to get a reasonable estimate for the excitonic bandgap. If not possible to do so, the modulation spectroscopy method or "inflection point" scheme will likely be better than Tauc-plot.

6 Summary and Conclusions

A brief history of studying the (Wannier) excitons in semiconductors is highlighted using a few familiar semiconductors. Various examples are given to clarify some myths about the excitonic effects in semiconductors.

Because, by definition, the excitonic bandgap E_{ex} is below the single-electron bandgap E_g, conceptually, it is inappropriate to use the Tauc-plot scheme to extract the bandgap E_g. Thus, the excitonic bandgap, ideally the energy threshold of the optical absorption in a direct bandgap material, should be used as the fundamental bandgap. However, if the material is so much perturbed by extrinsic effects, such as doping, alloying, defects, *etc.*, such that a reasonable estimate of the excitonic transition energy is not practically feasible,

using the modulation spectroscopy method or inflection point scheme will likely be better than Tauc-plot.

Response Letter is available for this paper at: http://cjl.lightpublishing.cn/thesisDetails#10.37188/CJL.EN20240013

References:

[1] BASSANI F, PARRAVICINI G P. *Electronic States and Optical Transitions in Solids* [M]. Oxford: Pergamon Press, 1975.

[2] SCHAEFER S T, GAO S, WEBSTER P T, *et al*. Absorption edge characteristics of GaAs, GaSb, InAs, and InSb [J]. *J. Appl. Phys.*, 2020, 127(16): 165705.

[3] CALLAWAY J. Theory of scattering in solids [J]. *J. Math. Phys.*, 1964, 5(6): 783-798.

[4] TAUC J, GRIGOROVICI R, VANCU A. Optical properties and electronic structure of amorphous germanium [J]. *Phys. Status Solidi* B, 1966, 15(2): 627-637.

[5] WENDLANDT W W, HECHT H G. *Reflectance Spectroscopy* [M]. New York: Interscience Publishers, 1966.

[6] ELLIOTT R J. Intensity of optical absorption by excitons [J]. *Phys. Rev.*, 1957, 108(6): 1384-1389.

[7] MACFARLANE G G, MCLEAN T P, QUARRINGTON J E, *et al*. Direct optical transitions and further exciton effects in germanium [J]. *Proc. Phys. Soc.*, 1958, 71(5): 863-866.

[8] HAYASHI M, KATSUKI K. Absorption spectrum of cuprous oxide [J]. *J. Phys. Soc. Jpn.*, 1950, 5(5): 380B-381.

[9] KAZIMIERCZUK T, FRÖHLICH D, SCHEEL S, *et al*. Giant rydberg excitons in the copper oxide Cu_2O [J]. *Nature*, 2014, 514(7522): 343-347.

[10] HOBDEN M V, STURGE M D. The optical absorption edge of gallium arsenide [J]. *Proc. Phys. Soc.*, 1961, 78(4): 615-616.

[11] STURGE M D. Optical absorption of gallium arsenide between 0.6 and 2.75 eV [J]. *Phys. Rev.*, 1962, 127(3): 768-773.

[12] WEISBUCH C, BENISTY H, HOUDRÉ R. Overview of fundamentals and applications of electrons, excitons and photons in confined structures [J]. *J. Lumin.*, 2000, 85(4): 271-293.

[13] SELL D D. Resolved free-exciton transitions in the optical-absorption spectrum of GaAs [J]. *Phys. Rev.* B, 1972, 6(10): 3750-3753.

[14] ZHANG Y, FLUEGEL B, HANNA M C, *et al*. Effects of heavy nitrogen doping in Ⅲ-Ⅴ semiconductors-how well does the conventional wisdom hold for the dilute nitrogen "Ⅲ-Ⅴ-N alloys"? [J]. *Phys. Status Solidi* C, 2003, 240(2): 396-403.

[15] LEIDERER H, SUPRITZ A, SILBERBAUER M, *et al*. Reflectivity and absorption of thin ZnTe epilayers near the exciton-polariton [J]. *Semicond. Sci. Technol.*, 1991, 6(9A): A101-A104.

[16] ZHANG Y, DALPIAN G M, FLUEGEL B, *et al*. Novel approach to tuning the physical properties of organic-inorganic hybrid semiconductors [J]. *Phys. Rev. Lett.*, 2006, 96(2): 026405.

[17] ZHANG Y, FLUEGEL B, HANNA M, *et al*. Electronic structure near the band gap of heavily nitrogen doped GaAs and GaP [J]. *MRS Online Proc. Libr.*, 2001, 692: 211.

[18] VARFOLOMEEV A V, SEISYAN R P, YAKIMOVA R N. Observation of the exciton structure in the fundamental absorption edge of indium arsenide crystals [J]. *Sov. Phys. Semicond.*, 1975, 9(4): 530.

[19] KANSKAYA L M, KOKHANOVSKIF S I, SEISYAN R P. Detection of the exclton structure of the absorption edge of indium antimonide crystais [J]. *Sov. Phys. Semicond.*, 1979, 13(12): 1420.

[20] GOBELI G W, FAN H Y. *Semiconductor Research, Second Quarterly Report* [M]. Lafayette, Indiana: Purdue Univ., 1956.

[21] JOHNSON E J. Absorption near the fundamental edge [J]. *Semicond. Semimetals*, 1967, 3: 153-258.

[22] KITTEL C. *Introduction To Solid State Physics* [M]. 8th ed. Hoboken: John Wiley & Sons, Inc, 2005.

[23] MUTH J F, LEE J H, SHMAGIN I K, *et al*. Absorption coefficient, energy gap, exciton binding energy, and recombination lifetime of GaN obtained from transmission measurements [J]. *Appl. Phys. Lett.*, 1997, 71(18): 2572-2574.

[24] ZHAO G Y, ISHIKAWA H, JIANG H, *et al*. Optical absorption and photoluminescence studies of n-type GaN [J]. *Jpn.*

J. Appl. Phys., 1999, 38(9A): L993-L995.

[25] ASPNES D E. Third-derivative modulation spectroscopy with low-field electroreflectance [J]. *Surf. Sci.*, 1973, 37: 418-442.

[26] CARDONA M. Modulation spectroscopy of semiconductors [M]. MADELUNG O. *Festkörperprobleme* 10. Berlin: Springer, 1970: 125-173.

[27] SHEN H, POLLAK F H. Generalized Franz-Keldysh theory of electromodulation [J]. *Phys. Rev.* B, 1990, 42(11): 7097-7102.

[28] DHERE R G, ZHANG Y, ROMERO M J, *et al*. Investigation of junction properties of CdS/CdTe solar cells and their correlation to device properties [C]. 2008 33*rd IEEE Photovoltaic Specialists Conference*, *San Diego*, 2008: 1-5.

[29] SHIRAYAMA M, KADOWAKI H, MIYADERA T, *et al*. Optical transitions in hybrid perovskite solar cells: ellipsometry, density functional theory, and quantum efficiency analyses for $CH_3NH_3PbI_3$ [J]. *Phys. Rev. Appl.*, 2016, 5(1): 014012.

[30] ZHANG F, CASTANEDA J F, CHEN S S, *et al*. Comparative studies of optoelectrical properties of prominent PV materials: halide perovskite, CdTe, and GaAs [J]. *Mater. Today*, 2020, 36: 18-29.

[31] KUDMAN I, SEIDEL T. Absorption edge in degenerate *p*-type GaAs [J]. *J. Appl. Phys.*, 1962, 33(3): 771-773.

[32] SHI D, ADINOLFI V, COMIN R, *et al*. Low trap-state density and long carrier diffusion in organolead trihalide perovskite single crystals [J]. *Science*, 2015, 347(6221): 519-522.

[33] DONG Q F, FANG Y J, SHAO Y C, *et al*. Electron-hole diffusion lengths > 175 μm in solution-grown $CH_3NH_3PbI_3$ single crystals [J]. *Science*, 2015, 347(6225): 967-970.

[34] SEBASTIAN M, PETERS J A, STOUMPOS C C, *et al*. Excitonic emissions and above-band-gap luminescence in the single-crystal perovskite semiconductors $CsPbBr_3$ and $CsPbCl_3$ [J]. *Phys. Rev.* B, 2015, 92(23): 235210.

[35] SAOUMA F O, STOUMPOS C C, KANATZIDIS M G, *et al*. Multiphoton absorption order of $CsPbBr_3$ as determined by wavelength-dependent nonlinear optical spectroscopy [J]. *J. Phys. Chem. Lett.*, 2017, 8(19): 4912-4917.

[36] KRÜCKEMEIER L, RAU U, STOLTERFOHT M, *et al*. How to report record open-circuit voltages in lead-halide perovskite solar cells [J]. *Adv. Energy Mater.*, 2020, 10(1): 1902573.

[37] GREEN M A, JIANG Y J, SOUFIANI A M, *et al*. Optical properties of photovoltaic organic-inorganic lead halide perovskites [J]. *J. Phys. Chem. Lett.*, 2015, 6(23): 4774-4785.

[38] ZIFFER M E, MOHAMMED J C, GINGER D S. Electroabsorption spectroscopy measurements of the exciton binding energy, electron-hole reduced effective mass, and band gap in the perovskite $CH_3NH_3PbI_3$ [J]. *ACS Photonics*, 2016, 3(6): 1060-1068.

[39] ZHONG H, PAN F J, YUE S, *et al*. Idealizing tauc plot for accurate bandgap determination of semiconductor with ultraviolet-visible spectroscopy: a case study for cubic boron arsenide [J]. *J. Phys. Chem. Lett.*, 2023, 14(29): 6702-6708.

张勇(1960-),男,福建福州人,博士,讲席教授,1994 年于 Dartmouth College 获得博士学位,主要从事半导体光电材料物理与器件物理的研究。
E-mail: yong. zhang@charlotte. edu